Influence of River Discharge and Dredging on Tidal Wave Propagation: Modaomen Estuary Case

Article *in* Journal of Hydraulic Engineering · October 2012

DOI: 10.1061/(ASCE)HY.1943-7900.0000594

5 authors, including:

Huayang Cai
Sun Yat-Sen University
71 PUBLICATIONS **982** CITATIONS
SEE PROFILE

Hubert H. G. Savenije
Delft University of Technology
462 PUBLICATIONS **23,282** CITATIONS
SEE PROFILE

Influence of River Discharge and Dredging on Tidal Wave Propagation: Modaomen Estuary Case

Huayang Cai[1]; Hubert H. G. Savenije[2]; Qingshu Yang[3]; Suying Ou[4]; and Yaping Lei[5]

Abstract: Dredging and flow reduction in the Modaomen Estuary in China have had a measurable impact on tidal propagation and damping. This paper includes an assessment of the impacts of these human interventions through the use of a new analytical hydraulic model procedure. The model calculates tidal propagation and damping as a function of bathymetry and river discharge through a simple iterative procedure with explicit analytical equations. The results obtained are accurate and allow both an analysis of the historic development and a sensitivity analysis to assess the effect of possible further dredging and flow reduction. Particularly in the upper reaches of the estuary, tidal damping and wave celerity are sensitive to dredging and flow reduction. Historic analysis shows that due to these activities, since 1993, the tidal amplitude in the Modaomen Estuary has increased by more than 0.1 m, while the travel time of the tidal wave has decreased by 30 min in the middle part of the estuary and up to 80 min in the upper reaches. In the future, the tidal amplitude and the wave celerity will increase even further if flow reduction and dredging continue. Moreover, this development would increase the risk of salinization in the estuary and facilitate the inland propagation of storm surges. **DOI: 10.1061/(ASCE)HY.1943-7900.0000594.**

CE Database subject headings: Analytical techniques; Tidal currents; Wave propagation; Dredging; China; Estuaries.

Author keywords: Analytical model; Deepening; Tidal amplitude; Wave celerity.

Introduction

Estuaries comprise intensively used coastal areas that are most at risk from human activities such as, for example, dam construction, land reclamation, dredging, flow reduction. While the effects of these human interventions on estuaries have been studied extensively, most studies have been confined to changes in sediment properties (Bai et al. 2003; Hossain et al. 2004; Kim et al. 2006; Li 2010), morphology (Barusseau et al. 1998; Blott et al. 2006; Xie et al. 2009; Jeuken and Wang 2010), ecosystems (Edgar and Barrett 2000; Byun et al. 2005; Smith et al. 2006; 2010), and analysis of the hydrological regime (Hoa et al. 2007; Luo et al. 2007; Liria et al. 2009; Zhang et al. 2010). Only few studies analyzed the effects of flow reduction and dredging on tidal wave propagation in estuaries (e.g., Godin 1999; Horrevoets et al. 2004). However, knowledge of the impacts of these human interventions on tidal wave propagation is important as they affect the aquatic environment of an estuary and the potential use of water resources. In addition, they have a direct relation to salt intrusion and storm surge propagation into the estuary. In the engineering community, many impact studies have been done throughout the world that make use of numerical models. However, for an enhanced understanding of human impacts on estuarine processes, numerical models are not much more than black boxes. Hence, an objective of this study is to provide an analytical instrument to assess the effect of flow reduction and dredging on tidal wave propagation in estuaries, with the Modaomen Estuary as an example.

The Modaomen Estuary, which has the largest flood discharge and sediment transport rate in the Pearl River system (Fig. 1), has been significantly affected by anthropogenic activities. In particular, since the 1980s the hydrology and morphology of the Modaomen Estuary has experienced uncontrolled and uneven sand excavation, which substantially changed the flow division between the various water courses while the degradation of the riverbed changed the dynamics of the tide and increased the salt intrusion (Luo et al. 2007). Metropolitan areas experience saline water intrusion especially in the dry season, and this phenomenon has become more serious in recent years (Zhang et al. 2009). The estuary also occasionally suffers from storm surges, which can cause serious flooding in the coastal area, as was the case in 2008. The concern is that dredging activities may enhance the propagation of storm surges into the interior. To assess these hazards, for the first time an analytical model has been developed to analyze the impacts of dredging and flow reduction on tidal wave propagation; the model has been applied to and tested on the historical developments in the Modaomen Estuary.

Since natural estuaries have converging topography, many researchers have studied the behavior of tidal wave propagation in convergent estuaries, generally with an exponentially varying cross section. Most researchers linearized the one-dimensional hydrodynamic equations by scaling, e.g., Jay (1991), Friedrichs and Aubrey (1994), Lanzoni and Seminara (1998), Toffolon and Savenije (2011) Savenije (1998, 2001, 2005), and Savenije et al. (2008) did not linearize the friction term and used a Lagrangian

[1]Ph.D. Student, Dept. of Water Management, Faculty of Civil Engineering and Geosciences, Delft Univ. of Technology, Stevinweg 1, P.O. Box 5048, 2600 GA Delft, The Netherlands (corresponding author). E-mail: h.cai@tudelft.nl

[2]Professor, Dept. of Water Management, Faculty of Civil Engineering and Geosciences, Delft Univ. of Technology, Stevinweg 1, P.O. Box 5048, 2600 GA Delft, The Netherlands.

[3]Associate Professor, Institute of Estuarine and Coastal Research, Sun Yat-sen Univ., Guangzhou, 510275, China.

[4]Lecturer, Institute of Estuarine and Coastal Research, Sun Yat-sen Univ., Guangzhou, 510275, China.

[5]Lecturer, Institute of Estuarine and Coastal Research, Sun Yat-sen Univ., Guangzhou, 510275, China.

Note. This manuscript was submitted on August 15, 2011; approved on March 20, 2012; published online on March 22, 2012. Discussion period open until March 1, 2013; separate discussions must be submitted for individual papers. This paper is part of the ***Journal of Hydraulic Engineering***, Vol. 138, No. 10, October 1, 2012. © ASCE, ISSN 0733-9429/2012/10-885-896/$25.00.

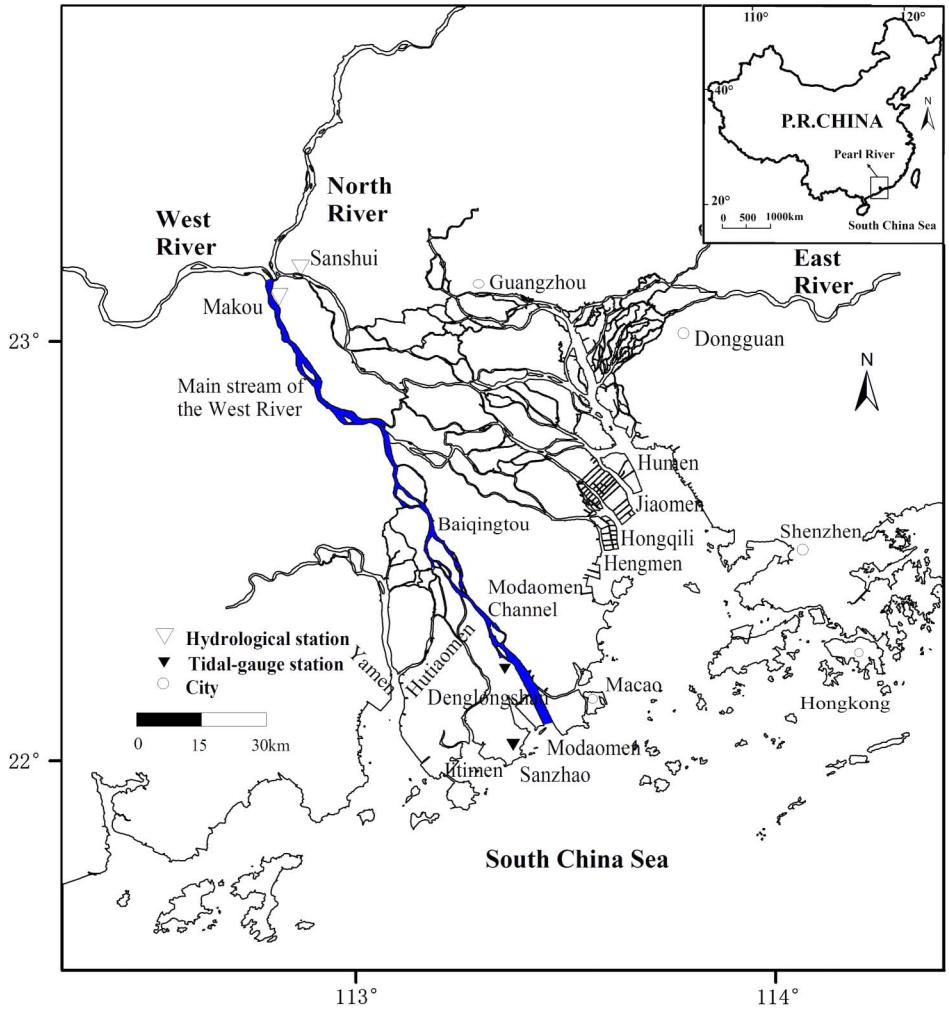

Fig. 1. Map of Pearl River system indicating Modaomen Estuary consisting of the main stream of West River and Modaomen Channel

approach to derive analytical equations for tidal wave propagation in estuaries of infinite length (long in relation to the wave length). Horrevoets et al. (2004), building on this work, included the effect of river discharge on tidal damping. This paper uses the explicit analytical equations of Savenije et al. (2008) and combines these with the equations of Horrevoets et al. (2004) to account for the effects of flow reduction and dredging on tidal damping and wave propagation.

In the following sections, a general procedure is described for solving these equations, after which the procedure is applied and tested in the Modaomen Estuary. Finally, a historical analysis indicates the effects that human interventions have had on tidal wave propagation in the Modaomen Estuary and the risk that the region runs if present trends continue.

Analytical Model for Tidal Wave Propagation Accounting for River Discharge

For given topography, friction, and tidal amplitude at the downstream boundary, the velocity amplitude, wave celerity, tidal damping, and phase lag can be computed with the analytical model derived by Savenije et al. (2008) However, in the derivation of this model, river discharge is assumed to be small compared to tidal flow. It is important to note that this assumption is only valid in the lower part of an estuary (Horrevoets et al. 2004). In the upstream, where the cross-sectional area approaches that of the river, the river discharge can have a considerable effect on tidal damping. In what follows, an expanded dimensionless equation for tidal damping is presented that accounts for the effect of river discharge. Subsequently, we present a new analytical procedure to assess the effects of human interventions in estuaries (e.g., by dredging or flow reduction).

The main geometric parameters of alluvial estuaries (the tidal average cross-sectional area, width, and depth) can be described by exponential functions along the estuary axis (Savenije 2005):

$$\bar{A} = \bar{A}_0 \exp\left(-\frac{x}{a}\right) \tag{1}$$

$$\bar{B} = \bar{B}_0 \exp\left(-\frac{x}{b}\right) \tag{2}$$

$$\bar{h} = \bar{h}_0 \exp\left(-\frac{x}{d}\right) \tag{3}$$

where $\bar{A}$, $\bar{B}$, and $\bar{h}$ = tidal average cross-sectional area, width, and depth; $\bar{A}_0$, $\bar{B}_0$, and $\bar{h}_0$ = tidal average cross-sectional area, width, and depth at the estuary mouth; x = distance from the estuary mouth; and a, b, and d are convergence lengths of the cross-sectional area, width, and depth, respectively. It

J. Hydraul. Eng. 2012.138:885-896.

follows from $\bar{A} = \bar{B}\,\bar{h}$ that $d = ab/(b-a)$. The parameters of the equation are obtained by regression on bathymetric data.

The basic one-dimensional equations describing the tidal dynamics in an estuary are the momentum and continuity equations (e.g., Savenije 2005), which read

$$\frac{\partial U}{\partial t} + U\frac{\partial U}{\partial x} + g\frac{\partial h}{\partial x} + gI_b + gn^2\frac{U|U|}{h^{4/3}} = 0 \tag{4}$$

$$r_s\frac{\partial A}{\partial t} + \frac{\partial Q}{\partial x} = 0 \tag{5}$$

where t = time; U = cross-sectional average flow velocity; g = acceleration due to gravity; n = Manning's coefficient; I_b = bottom slope; and Q = tidal flow discharge. The ratio between the storage width and the stream width is r_s (assuming constant during one tidal cycle).

The system is forced by a sinusoidal tidal wave with a tidal period T and a frequency $\omega = 2\pi/T$. As the wave propagates into the estuary, it has a wave celerity c, an amplitude of the tidal water level variation η, a tidal velocity amplitude v, and a phase lag ϵ, defined as the phase difference between high water (HW) and high water slack (HWS) [or between low water (LW) and low water slack (LWS)]. After scaling of Eqs. (4) and (5), five dimensionless variables can be found: the estuary shape number γ, the friction number χ, the velocity number μ, the celerity number λ, and the damping number for tidal amplitude δ (Savenije et al. 2008), where γ and χ are the independent variables, while ϵ, μ, λ, and δ are the dependent variables. These dimensionless variables are defined as

$$\gamma = \frac{c_0}{\omega a} \tag{6}$$

$$\chi = r_s f\frac{c_0}{\omega\bar{h}}\zeta \tag{7}$$

$$\mu = \frac{1}{r_s}\frac{v\bar{h}}{\eta c_0} \tag{8}$$

$$\lambda = \frac{c_0}{c} \tag{9}$$

$$\delta = \frac{1}{\eta}\frac{\mathrm{d}\eta}{\mathrm{d}x}\frac{c_0}{\omega} \tag{10}$$

where c_0 = classical wave celerity of a frictionless progressive wave; $\bar{h}$ = tidal average depth of flow; f = dimensionless friction factor; and ζ = dimensionless tidal amplitude defined as

$$c_0 = \sqrt{g\bar{h}/r_s} \tag{11}$$

$$f = \frac{gn^2}{\bar{h}^{1/3}}\left[1 - \left(\frac{4}{3}\zeta\right)^2\right]^{-1} \tag{12}$$

$$\zeta = \frac{\eta}{\bar{h}} \tag{13}$$

Making use of these dimensionless parameters, Savenije et al. (2008) derived four dimensionless equations on the basis of the equations for the phase lag (Savenije 1992, 1993), for tidal damping (Savenije 1998, 2001), and for wave propagation (Savenije and Veling 2005):

$$\tan(\epsilon) = \frac{\lambda}{\gamma - \delta} \tag{14}$$

$$\mu = \frac{\sin(\epsilon)}{\lambda} = \frac{\cos(\epsilon)}{\gamma - \delta} \tag{15}$$

$$\delta = \frac{\mu^2}{\mu^2 + 1}(\gamma - \chi\mu^2\lambda^2) \tag{16}$$

$$\lambda^2 = 1 - \delta(\gamma - \delta) \tag{17}$$

Eqs. (14), (15), and (17) are commonly used in tidal hydraulics for the case of an infinite channel (e.g., Toffolon and Savenije 2011; Van Rijn 2011), but Eq. (16) is different from the commonly used damping equation with a linearized friction term. The equation used here, developed by Savenije (1998), uses nonlinear friction, whereby the differential equations are conditioned for HW and LW. This procedure is also followed in Appendix I. The advantage of this set of Eqs. (14)–(17) is that they can be solved analytically with a fully explicit solution, provided the effect of river discharge is negligible (Savenije et al. 2008).

The next step is to account for river discharge. For this purpose the new dimensionless river discharge term φ is introduced:

$$\varphi = \frac{Q_f}{Av\sin(\epsilon)} \tag{18}$$

where Q_f is the river discharge.

Rewriting the equations of Horrevoets et al. (2004) for tidal damping with a measurable effect of river discharge leads to a new expression for the tidal damping number δ', where two zones are distinguished depending on the value of φ (Appendix I).

In the downstream zone where $\varphi \le 1$,

$$\delta' = \frac{\mu^2}{\mu^2(\theta - r_s\varphi\zeta) + 1}\left[\theta\gamma - \chi\mu^2\lambda^2\left(1 + \varphi^2 + \frac{8}{3}\varphi\zeta\right)\right] \tag{19}$$

In the upper zone where $\varphi > 1$,

$$\delta' = \frac{\mu^2}{\mu^2(\theta - r_s\varphi\zeta) + 1}\left[\theta\gamma - \chi\mu^2\lambda^2\left(\frac{4}{3}\zeta + \frac{4}{3}\varphi^2\zeta + 2\varphi\right)\right] \tag{20}$$

with

$$\theta = 1 - \varphi\left(\sqrt{1+\zeta} - 1\right) \tag{21}$$

The difference between Eqs. (19) and (16) is in the terms containing φ. If $Q_f = 0$ (implying that $\varphi = 0$), then they are identical.

With Eqs. (19) and (20) to replace Eq. (16), an analytical model can be made to access the effect of river discharge and bathymetry on tidal damping and propagation. Fig. 2 is a flow chart that shows the calculation process. Initially we assume $Q_f = 0$, after which initial values are computed for the velocity number μ, celerity number λ, damping number δ, and phase lag ϵ. Taking into account the effect of river discharge Q_f, the revised damping number δ' is calculated using Eqs. (19) and (20). Subsequently, using δ' for δ, the new celerity number λ', phase lag ϵ', and velocity number μ' can be computed using Eqs. (17), (14), and (15), followed by a new estimate of δ'. This process is repeated until the result is stable. Finally, the tidal amplitude along the estuary can be calculated through numerical integration of δ'.

J. Hydraul. Eng. 2012.138:885-896.

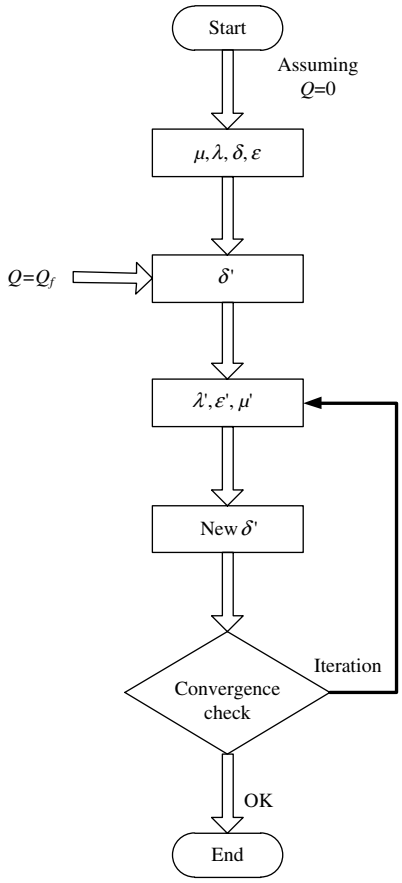

Fig. 2. Calculation process for tidal damping and wave celerity in an estuary as a result of river discharge

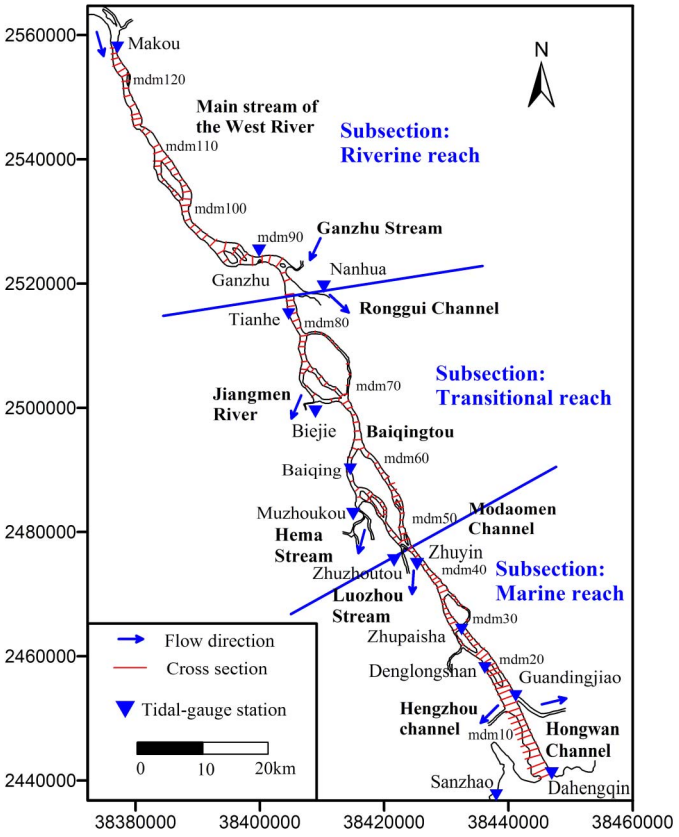

Fig. 3. Sketch indicating location of cross sections and reference points in Modaomen Estuary

Modaomen Estuary

Overview of Modaomen Estuary

The Modaomen Estuary is located in the downstream portion of the West River, one of the three major rivers (West River, North River, and East River) entering the Pearl River Delta (Fig. 1). After entering the delta area, the Modaomen Estuary passes through the main stream of the West River from Makou to Baiqingtou and finally reaches the Modaomen Channel from Baiqingtou to the estuary mouth. Among the eight outlets in the Pearl River system that discharge freshwater into the South China Sea, the Modaomen Estuary carries the largest portion of river discharge. At the upstream boundary of the estuary, on the basis of the river discharge data at Makou from 1950 to 2009, the mean annual runoff is $7,115\ m^3/s$, with an average river discharge of $10,900\ m^3/s$ during the wet season (April–September) and $3,329\ m^3/s$ during the dry season. The Modaomen Estuary experiences a microscale tide, with an annual mean tidal range of 1.11 m at Sanzhao Station, decreasing to 0.86 m at Denglongshan Station. It has an irregular semidiurnal character, with the amplitude of the four main tidal constituents M_2, S_2, K_1, and O_1 of 0.43, 0.18, 0.42, and 0.37 m at Sanzhao Station, respectively (Gong and Shen 2011).

Shape of Modaomen Estuary

On the basis of topographic maps of the Pearl River surveyed in 1999, and a digital elevation model (DEM) of the Modaomen Estuary, 126 cross sections (Fig. 3) have been extracted to obtain the cross-sectional area, width, and depth of each cross section. Fig. 4 shows the geometry of the Modaomen Estuary, where the tidal average cross-sectional area, width, and depth are plotted on semilogarithmic paper. Fig. 4 shows that the estuary can be divided into three distinct reaches: the downstream marine reach ($x = 0$–43 km, mdm1-mdm46), the transitional reach ($x = 43$–91 km, mdm47-mdm85), and the upstream riverine reach ($x = 91$–145 km, mdm86-mdm126), where two distinct points of division can be identified. The corresponding regions are indicated in Fig. 3. In general, the reach from Makou to Baiqingtou is called the main stream of the West River ($x = 59$–145 km), while the remaining subsection is called the Modaomen Channel ($x = 0$–59 km). The convergence lengths of cross-sectional area and width as well as tidal average depth of flow in each subsection are summarized in Table 1. Parallel branches separated by islands have been combined, as suggested by Nguyen and Savenije (2006).

Discharge in Modaomen Estuary

The model has been calibrated by comparing the calculated tidal amplitude and travel time of tidal wave in the Modaomen Estuary to measurements observed during February 7–16, 2001. At the upstream end of the estuary ($x = 145$ km) there is a hydrological station (Makou Station) where a river discharge of $2,259\ m^3/s$ was observed on February 8–9, 2001 (spring tide), $1,895\ m^3/s$ on February 11–12, 2001 (transition period), $1,630\ m^3/s$ on February 14–15, 2001 (neap tide) (Fig. 5). We assume that the river discharge is constant during a specific tidal cycle, which is a reasonable assumption for our tidally averaged analytical model. To assess the effect of river discharge on tidal wave propagation, it is necessary to determine the river discharge distribution over the branches of the Modaomen Estuary. Since the current model can only deal

J. Hydraul. Eng. 2012.138:885-896.

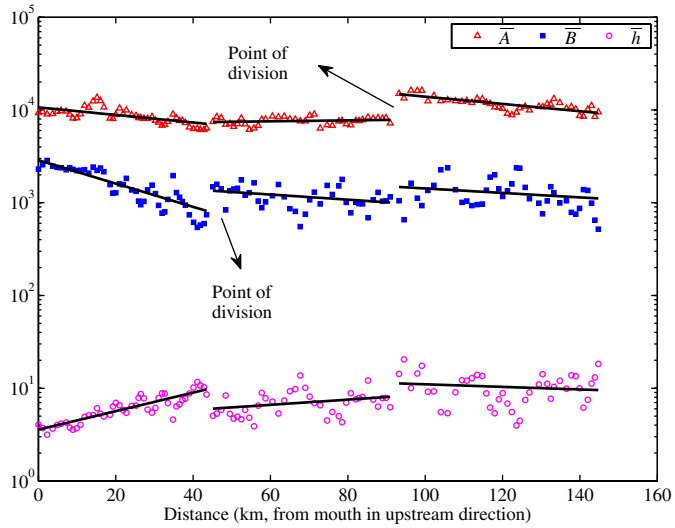

Fig. 4. Semilogarithmic plot of cross-sectional area $\bar{A}(\mathrm{m}^2)$, width $\bar{B}(\mathrm{m})$, and average depth $\bar{h}(\mathrm{m})$ along estuary axis with trend lines

Table 1. Shape Characteristics of Modaomen Estuary

Subsection	Area convergence length a (km)	Width convergence length b (km)	Depth convergence length d (km)	Tidal average depth of flow h (m)
mdm1-mdm46	106	35	−52	6.3
mdm47-mdm85	−833	159	−134	7.0
mdm86-mdm126	110	179	285	10.3

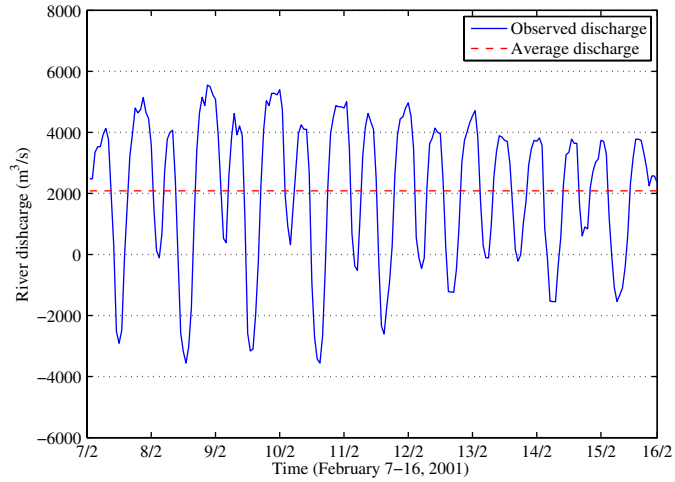

Fig. 5. Variation in river discharge at Makou hydrological station observed during February 7–16, 2001

with single channel or multiple channels constrained in one main branch, the possible effect of side channels (e.g., Ronggui Channel in Fig. 3) on tidal wave propagation in the main branch are taken into account by specifying a particular Q_f in the various reaches of the estuary. The observed river discharge distribution along the branches of the Modaomen Estuary during February 7–16, 2001 is summarized in Table 2, with a plus sign for flows entering the main branch of the estuary and a minus sign for those leaving. The distribution of river discharge at downstream reaches does not add up to 100% at Makou (there is a −38.1% difference in Table 2),

Table 2. Mean River Discharge Distribution Observed in Modaomen Estuary During February 7–16, 2001

Tidal-gauge station	Channel	Percentage	Daily river discharge (m^3/s)
Makou	Main stream of West River	100	+2,085
Tianhe	Main stream of West River	47	+971
Nanhua	Ronggui Channel	37	−779
Beijie	Jiangmen River	2.7	−56
Muzhoukou	Hema stream	10	−214
Zhuzhoutou	Luozhou stream	2.6	−54
Denglongshan	Modaomen Channel	9.6	+201

primarily because of the intake of water for drinking, irrigation, industry, and other activities along the estuary. In the current model, this part of water loss was not taken into account, but it is worth verifying it with available data (e.g., intake of water by waterworks along the estuary) in the future. We also neglected the inflow of Ganzhu Stream (Fig. 3) since its inflow is small and can be negligible compared with the inflow of Makou. The input data are summarized in Table 3, where we observe a mixed tide with variable tidal periods, which account for the variation in the timing between successive low waters.

Effect of River Discharge on Tidal Wave Propagation in Modaomen Estuary

Model Calibration

First, the analytical model is applied without taking account of the effect of river discharge (allowing $Q_f = 0$ or $\varphi = 0$) to be compared to observations made in the Modaomen Estuary on February 8–9, 11–12, and 14–15, 2001. The model uses the Modaomen Estuary geometry presented in Table 1. The length of the estuary is $L = 145$ km. The cross-sectional area and width at the estuary mouth are $A_0 = 9325\ \mathrm{m}^2$ and $B_0 = 2.3$ km. The models were forced with a sinusoidal tidal wave as specified in Table 3. The calibration parameters, particularly the storage width ratio r_s and Manning's coefficient n, are presented in Table 4. In general, the storage width ratio r_s ranges between 1 and 2 (Savenije 2005), whereas Manning's coefficient n in estuaries typically varies within a range of between 0.017 and 0.06 $\mathrm{m}^{-1/3}$s (Savenije 2001; Punt et al. 2003).

In Table 5, the results of the analytical model are compared to the observed tidal amplitude and travel time in the Modaomen Estuary during spring tide on February 8–9, 2001 moderate tide on February 11–12, 2001 and neap tide on February 14–15, 2001. The model fits the observations of tidal amplitude very well, except for at Guadingjiao Station near the estuary mouth.

Table 3. Input Used for Analytical Model

Station	Period	Tidal amplitude at seaward boundary (m)	Tidal period (s)	Average river discharge at Makou (m^3/s)
Sanzao	February 8–9, 2001	1.31	92,400	2,259
	February 11–12, 2001	0.97	90,600	1,895
	February 14–15, 2001	0.49	90,000	1,630
Dahengqin	December 5–6, 2002	1.09	88,500	2,570
	December 8–9, 2002	0.86	87,300	1,986
	December 11–12, 2002	0.59	91,800	1,920

J. Hydraul. Eng. 2012.138:885-896.

Table 4. Parameters Used for Analytical Model

Subsection	Storage width ratio r_s	Manning's coefficient n ($m^{-1/3}s$) Without taking account of river discharge	Manning's coefficient n ($m^{-1/3}s$) Considering river discharge
mdm1-mdm46	1.2	0.031	0.031
mdm47-mdm85	1.1	0.018	0.018
mdm86-mdm126	1.0	0.052	0.02

The reason for the deviation at Guadingjiao Station is probably due to the existence of two side channels (Hezhou Channel and Hongwan Channel) (Fig. 3). For propagation of the tidal wave, the overall result is good, although the results for moderate tide and neap tide show some deviations.

Subsequently the system of equations is solved taking river discharge into account (with $\varphi > 0$). It appears that the iterative process presented in Fig. 2 converges already after the first iteration and that accurate estimates can be obtained. The calibrated Manning's coefficients resulting from this model are also presented in Table 4.

In Fig. 6 the damping numbers are shown for the case with and without river discharge. In the downstream end of the estuary the models are almost identical but perform differently in the upper reach, where the effect of discharge is more strongly felt. As shown in Table 4, Manning's coefficient n in the upstream river is much more realistic if river discharge is considered. Apparently the error introduced by not accounting for the discharge could be compensated by increasing the friction in the upper reaches of the Modaomen Estuary. The unrealistically high roughness of 0.052 $m^{-1/3}s$ in the first model is an artifact of not considering river discharge. The roughness value of 0.02 $m^{-1/3}s$ is much more realistic and according to expectation in this riverine part of the estuary. From a physical point of view, the friction term in the new damping Eqs. (19) and (20), i.e., $\chi\mu^2\lambda^2\left(1+\varphi^2+\frac{8}{3}\varphi\zeta\right)$ for $\varphi \le 1$ and $\chi\mu^2\lambda^2\left(\frac{4}{3}\zeta+\frac{4}{3}\varphi^2\zeta+2\varphi\right)$ for $\varphi > 1$, is more reasonable, where the effects of river discharge can be taken into account through the dimensionless river discharge term φ and the friction term is increased with river discharge.

Fig. 7(a) shows the tidal amplitude along the Modaomen Estuary for different dates with corresponding river discharge and tidal amplitudes at the estuary mouth. It can be seen that the correspondence with observations is good, with a mean absolute error of tidal amplitude of spring tide 0.03 m, moderate tide 0.05 m, and neap tide 0.02 m, respectively (Table 6).

In Fig. 7(b–d) the travel time of the tidal wave for these situations is compared to the observed travel time. The lines for spring tide (February 8–9, 2001) are very good, but the lines for moderate tide (February 11–12, 2001) and neap tide (February 14–15, 2001)

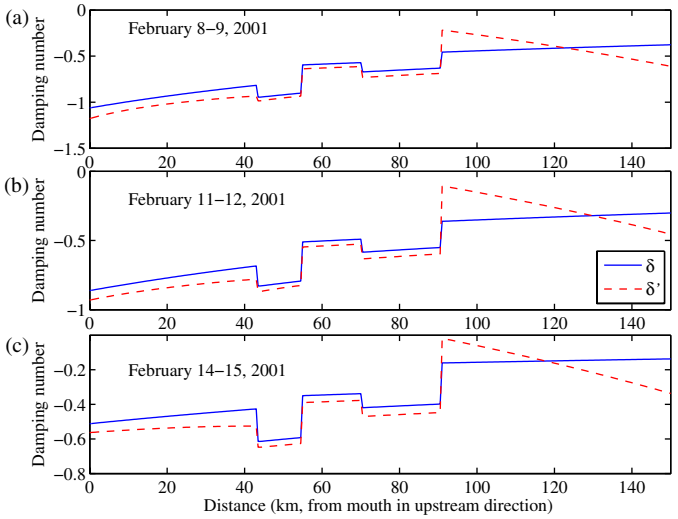

Fig. 6. Comparison of two analytical models to compute dimensionless damping number on (a) February 8–9, 2001; (b) February 11–12, 2001; (c) February 14–15, 2001; the drawn line represents the first model where discharge is neglected (δ); the dashed line represents the second model accounting for river discharge (δ')

show a deviation upstream from the point located 59 km from the mouth. The reason for the deviation should probably be sought in the effect of the storage width ratio r_s at different tidal amplitudes. This should be further explored in the future.

Model Verification

The model was further verified with the available data during a spring-neap tidal period on December 5–13, 2002 when a flow condition similar to calibrated period was observed. The input data are shown in Table 3, where the estuary mouth is located at Dahengqin Station (Fig. 3). Fig. 8 shows a comparison between the modeled calculations and the observations on different dates, with different river discharges. The calculated tidal amplitudes along the estuary agree well with measurements, with a mean absolute error of tidal amplitude of spring tide 0.04 m, moderate tide 0.05 m, and neap tide 0.03 m, respectively (Table 7). As can be seen from Fig. 8 and Table 7, the modeled tidal wave travel time generally followed the measurements. In general, through comparison with field data, it has been shown that the model reasonably reproduced the main features of the tidal wave propagation in the Modaomen Estuary. The model was then applied to investigate the influence of river discharge and dredging on tidal dynamics in the Modaomen Estuary.

Table 5. Calibration of Analytical Model without Taking Account of River Discharge

Tidal-gauge station	Mean absolute error of tidal amplitude (m) February 8–9, 2001	February 11–12, 2001	February 14–15, 2001	Mean absolute error of travel time of mean tide (min) February 8–9, 2001 HW	TA	LW	February 11–12, 2001 HW	TA	LW	February 14–15, 2001 HW	TA	LW
Guadingjiao	0.11	0.09	0.01	5	11	11	20	17	11	45	37	29
Denglongshan	0.04	0.04	0	10	1	0	19	13	5	3	9	14
Zhupaisha	0.04	0.06	0.01	22	12	10	5	6	11	5	0	5
Baiqing	0.04	0.07	0	19	0	3	27	23	10	26	37	45
Tianhe	0.05	0.06	0	16	4	6	24	21	8	17	46	72
Makou	0.05	0.05	0.05	23	2	0	40	31	11	32	55	75

J. Hydraul. Eng. 2012.138:885-896.

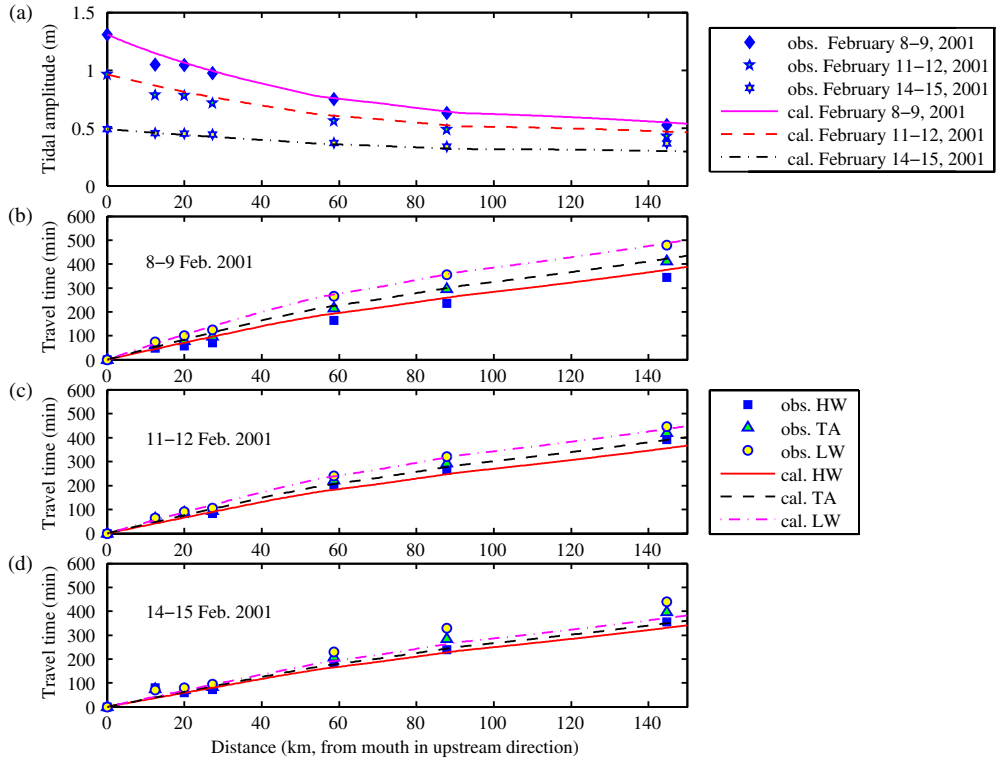

Fig. 7. Comparison of analytically calculated tidal amplitude (a) and travel time [including high water (HW), mean tide (TA), and low water (LW)] in Modaomen Estuary, considering river discharge, observed on (b) February 8–9, 2001; (c) February 11–12, 2001; (d) February 14–15, 2001

Table 6. Calibration of Analytical Model Considering River Discharge

Tidal-gauge station	Mean absolute error of tidal amplitude (m)			Mean absolute error of travel time of mean tide (min)								
				February 8–9, 2001			February 11–12, 2001			February 14–15, 2001		
	February 8–9, 2001	February 11–12, 2001	February 14–15, 2001	HW	TA	LW	HW	TA	LW	HW	TA	LW
Guadingjiao	0.10	0.08	0	3	8	8	18	15	9	43	36	27
Denglongshan	0.02	0.03	0.01	13	5	4	16	11	2	2	7	12
Zhupaisha	0.02	0.05	0.02	27	17	16	8	9	15	8	2	2
Baiqing	0.01	0.05	0.01	27	9	7	21	16	2	20	31	39
Tianhe	0.01	0.04	0.02	27	7	5	15	13	0	10	39	65
Makou	0.02	0.04	0.06	31	10	8	37	28	9	24	47	68

Sensitivity to River Discharge and Dredging

Sensitivity to River Discharge

The sensitivity experiments were perfomed with fixed parameters, i.e., assuming all calibration parameters (e.g., Manning's coefficient n, storage width ratio r_s) did not change. To investigate the effect of river discharge on tidal amplitude and travel time, the case of spring tide on February 8–9, 2001 is considered under different river discharge conditions. In Fig. 9 the ratio φ between the freshwater discharge and tidal flow amplitude at high water (HW) is presented for the Modaomen Estuary under different river discharge conditions. Subsequently, the sensitivity of damping and wave propagation to these ratios is assessed. As can be seen from Fig. 9, the largest effect is in the upstream part of the estuary. This implies that the river discharge becomes dominant from 91 km onward, i.e., the junction of Tianhe and Nanhua stations. For every increase in river discharge of 500 m^3/s, the ratio increases by approximately 53, 66, 81, and 99% upstream of Tianhe Station respectively. As can be seen from Fig. 10(a), tidal damping increases with river discharge, especially in the upper reach of the main stream of the West River. To be more precise, the tidal amplitude in the Modaomen Channel ($x = 0$–59 km) at a river discharge of 1,500 m^3/s decreases by 0.6, 1.3, 2.1, and 2.9% at a river discharge of 2,000 m^3/s, 2,500 m^3/s, 3,000 m^3/s, 3,500 m^3/s, respectively. Similarly, the tidal amplitude in the main stream of the West River ($x = 59$–145 km) decreases by 3.7, 7.1, 10.6, and 14.4%, respectively.

Fig. 10(b) shows that the wave celerity is decreased by river discharge primarily because of the increase in tidal damping. It can be seen that only in the upper reaches of the Modaomen Estuary, where the estuary gradually becomes riverine in character, does the wave celerity decrease significantly. According to the analytical model, the travel time of the tidal wave in the Modaomen Channel ($x = 0$–59 km) at a river discharge of 1,500 m^3/s increases by 1.2, 2.5, 4.2, and 5.9% at a river discharge of 2,000 m^3/s, 2,500 m^3/s, 3,000 m^3/s, and 3,500 m^3/s, respectively. Similarly, the tidal wave travel time in the main stream of the West River ($x = 59$–145 km) increases by 2.3, 4.5, 7.1, and 9.9%, respectively.

J. Hydraul. Eng. 2012.138:885-896.

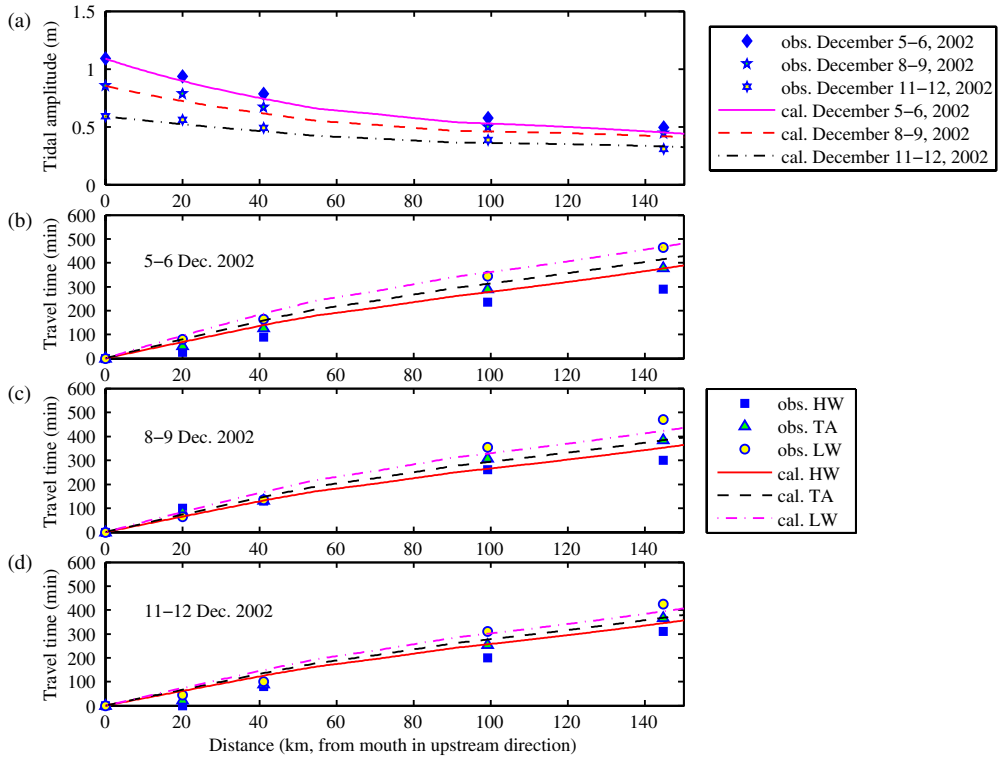

Fig. 8. Comparison of analytically calculated tidal amplitude (a) and travel time [including high water (HW), mean tide (TA), and low water (LW)] in the Modaomen Estuary, considering river discharge, observed on (b) December 5–6, 2002; (c) December 8–9, 2002; (d) December 11–12, 2002

Table 7. Verification of Analytical Model Considering River Discharge

Tidal-gauge station	Mean absolute error of tidal amplitude (m)			Mean absolute error of travel time of mean tide (min)								
				December 5–6, 2002			December 8–9, 2002			December 11–12, 2002		
	December 5–6, 2002	December 8–9, 2002	December 11–12, 2002	HW	TA	LW	HW	TA	LW	HW	TA	LW
Denglongshan	0.04	0.06	0.04	43	27	15	35	9	19	61	44	28
Zhuyin	0.04	0.05	0.03	47	30	20	0	13	31	43	44	46
Ganzhu	0.05	0.04	0.02	41	21	13	3	16	28	55	20	11
Makou	0.04	0.03	0.02	87	39	3	53	1	46	36	1	30

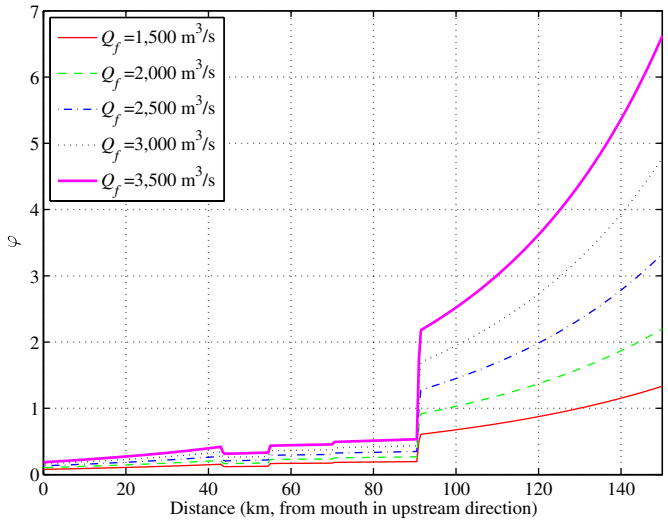

Fig. 9. Ratio of freshwater discharge Q_f to tidal flow amplitude at HW $[Av\ \sin(\epsilon)]$ as a function of distance for different river discharge (Makou Station) conditions

Sensitivity to Dredging

Taking the spring tide on February 8–9, 2001 with the same tidal amplitude at the estuary mouth and the same river discharge at the upstream end as the baseline case, the longitudinal variation of tidal amplitude under different riverbed elevations is presented in Fig. 11(a). The analytical model test shows that the tidal amplitude increases with a degradation of the riverbed and increasingly so further upstream. It is shown that the tidal amplitude in the Modaomen Channel ($x = 0$–59 km) would increase by 3.5, 6.8, 9.6, and 12.2% if the average depth increased by 0.5, 1.0, 1.5, and 2.0 m, respectively. In the main stream of the West River ($x = 59$–145 km), the increase of tidal amplitude is much more significant, with 8.6, 16.8, 24.5, and 31.8% gains, respectively.

In Fig. 11(b) the propagation of the tidal wave in the Modaomen Estuary under different riverbed elevations is shown. As can be seen in Fig. 11(b), it is clear that the wave celerity is substantially increased by deepening the riverbed. Specifically, the travel time of the tidal wave in the Modaomen Channel ($x = 0$–59 km) would decrease by 7.8, 14.8, 20.8, and 26.0% if the average depth increased by 0.5, 1.0, 1.5, and 2.0 m, respectively. Similarly, the tidal wave travel time in the main stream of the West River

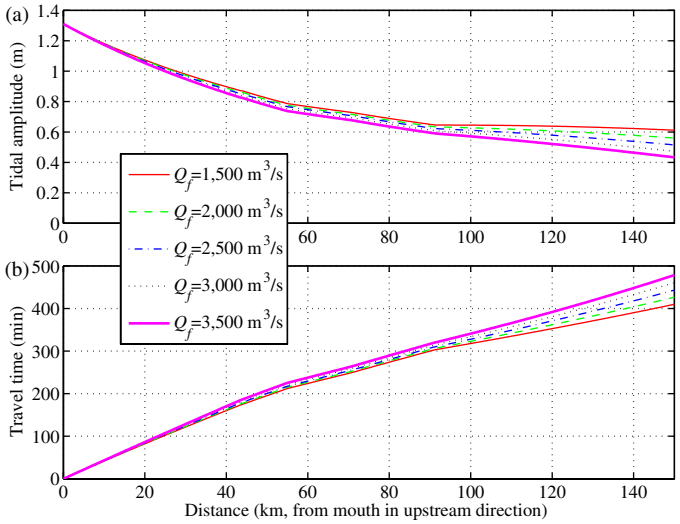

Fig. 10. Longitudinal variation of tidal amplitude (a) and propagation of tidal wave at mean tide (b) in Modaomen Estuary under different river discharge (Makou Station) conditions

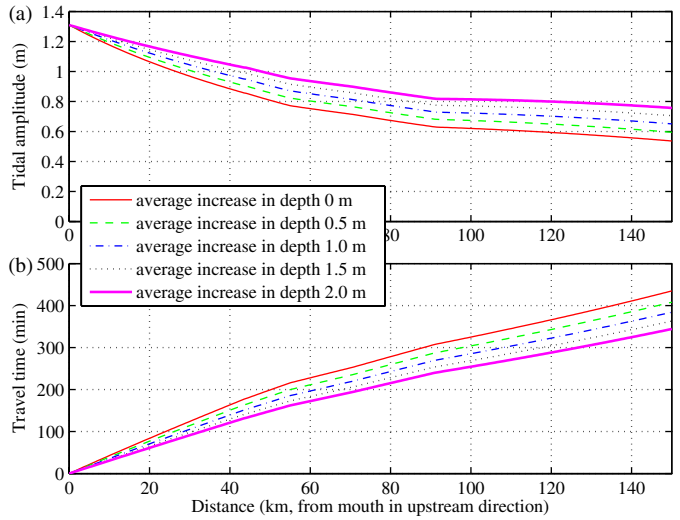

Fig. 11. Longitudinal variation of tidal amplitude (a) and propagation of the tidal wave at mean tide (b) in Modaomen Estuary under different riverbed degradation conditions

($x = 59$–145 km) would decrease by 6.5, 12.2, 17.3, and 21.8%, respectively.

Historic Analysis

Work by Luo et al. (2007) showed that uncontrolled sand excavation resulted in an average increase of the depth by 1.04 to 1.65 m in the main channels of the Modaomen Estuary between 1977 and 1999. In particular, the downstream marine subsection ($x = 0$–43 km), the transitional subsection ($x = 43$–91 km), and upstream riverine subsection ($x = 91$–145 km) deepened by 1.04, 1.42, and 1.65 m, respectively. Moreover, as a result of changed flow diversion upstream of Makou and Sanshui hydrological stations after 1993, the river discharge at Makou decreased by approximately 500 m^3/s compared to the discharge before 1993 in the dry season. As a result, our model simulations indicate that both the decrease in river discharge and the degradation of riverbed in the Modaomen Estuary resulted in a substantial increase in the

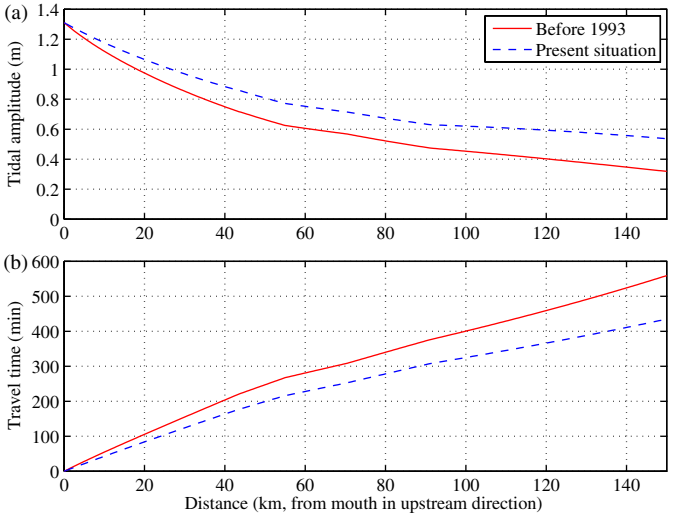

Fig. 12. Effect of recent dredging and flow reduction on the longitudinal variation of tidal amplitude (a) and propagation of tidal wave at mean tide (b) in Modaomen Estuary versus pre-1993 situation

tidal amplitude and a decrease in travel time. Fig. 12 indicates that since 1993 the tidal amplitude has increased by 0.10 m in the Modaomen Channel and 0.18 m in the main stream of the West River. Meanwhile, the travel time in the Modaomen Channel and the main stream of the West River decreased by 30 and 82 min, respectively. The results are in agreement with the previous study by Zhang et al. (2010), who identified the long-term change in tidal dynamics in the Pearl River Delta and concluded that the further upstream a part of the Modaomen Estuary is, the more obvious the change in trend. In fact, it can be seen that the friction term $\chi\mu^2\lambda^2(\frac{4}{3}\zeta + \frac{4}{3}\varphi^2\zeta + 2\varphi)$ in Eq. (19) for the upper reaches of the estuary is more sensitive to river discharge and deepening, which provides a reasonable explanation for the sensitivity to dredging and flow reduction in the upstream part of the estuary.

Conclusions

An iterative analytical method has been presented to calculate the effect of river discharge on tidal wave propagation in estuaries. This approach was tested in the Modaomen Estuary and proved to be efficient and accurate. Since the Modaomen Estuary is a typical riverine estuary, the influence of river discharge on tidal wave propagation is significant. The analytical model tests show that a reduction in river discharge and a degradation of the riverbed both lead to a significant increase in the tidal amplitude along the estuary axis, especially in the upper reaches of the Modaomen Estuary, and that the travel time of the tidal wave is reduced. Historical analysis shows that as a result of the flow reduction and dredging activities, since 1993, the tidal amplitude has increased by 0.10 m in the Modaomen Channel and 0.18 m in the main stream of the West River, whereas the tidal wave travel time decreased in these channels by 30 and 82 min, respectively.

This research demonstrates that the tidal amplitude along the estuary axis and the celerity of the wave propagation would increase even further as a result of the continuing decrease in river discharge and uncontrolled sand excavation. Because salt intrusion depends on both river discharge and depth, this development will lead to higher salinity levels in the estuary. More importantly, in line with the amplification of the tidal amplitude that is the result of dredging, further deepening will facilitate the penetration of

J. Hydraul. Eng. 2012.138:885-896.

storm surges into the estuary. Consequently, the Modaomen Estuary would be increasingly exposed to salt intrusion and to flooding from storm surges.

Appendix I. Derivation of Damping Equation Accounting for River Discharge

Using a Lagrangian approach for the analysis of tidal flow instead of the more common Eulerian one, as proposed by Savenije (2005), the continuity equation can be written as

$$\frac{dU}{dt} = r_s \frac{c}{h}\frac{dh}{dt} - \frac{cU}{a} + cU\frac{1}{\eta}\frac{d\eta}{dx} \tag{22}$$

The momentum equation can be written in a Lagrangian reference frame as well, which yields

$$\frac{dU}{dt} + g\frac{\partial h}{\partial x} + gI_b + gn^2\frac{U|U|}{h^{4/3}} = 0 \tag{23}$$

Combining Eqs. (22) and (23) and using $U = dx/dt$ yields

$$r_s\frac{cU}{gh}\frac{dh}{dx} - \frac{cU}{g}\left(\frac{1}{a} - \frac{1}{\eta}\frac{d\eta}{dx}\right) + \frac{\partial h}{\partial x} + I_b + n^2\frac{U|U|}{h^{4/3}} = 0 \tag{24}$$

Let us now consider the situation at HW and LW; then the following relations apply. Because the tidal range H ($H = 2\eta$) is the difference between h_{HW} and h_{LW},

$$2\frac{d\eta}{dx} = \frac{dh_{\mathrm{HW}}}{dx} - \frac{dh_{\mathrm{LW}}}{dx} \tag{25}$$

where $\bar{h}$ is the tidal average water level. Moreover, at HW and LW, by definition

$$\left.\frac{\partial h}{\partial t}\right|_{\mathrm{HW,LW}} = 0 \tag{26}$$

and hence

$$\frac{dh_{\mathrm{HW,LW}}}{dx} = \left.\frac{\partial h}{\partial x}\right|_{\mathrm{HW,LW}} \tag{27}$$

If the dimensionless tidal wave (scaled by the tidal range) is considered undeformed (which is the case when $\eta/\bar{h} \ll 1$), then the damping is symmetrical with respect to the tidal average water level $\bar{h}$, which may still have a residual slope $I = d\bar{h}/dx$

$$\frac{dh_{\mathrm{HW}}}{dx} + \frac{dh_{\mathrm{LW}}}{dx} \approx 2\frac{d\bar{h}}{dx} = 2I \tag{28}$$

with

$$h_{\mathrm{HW}} \approx \bar{h} + \eta \tag{29}$$

$$h_{\mathrm{LW}} \approx \bar{h} - \eta \tag{30}$$

These three approximations are not critical to the derivation and acceptable if $\eta/\bar{h} \ll 1$.

For the tidal velocity at HW and LW the following expression can be derived, where the river discharge Q_f is taken into account

$$U_{\mathrm{HW}} \approx \upsilon\sin(\epsilon) - \frac{Q_f}{A} \tag{31}$$

$$U_{\mathrm{LW}} \approx -\upsilon\sin(\epsilon) - \frac{Q_f}{A} \tag{32}$$

Further, we must realize that the celerities of propagation of the moment of HW (c_{HW}) and LW (c_{LW}) along the estuary are not equal (as a result of the different depths), but we may also assume that they are symmetrical compared to the tidal average wave celerity c, and hence that for small tidal amplitudes

$$\frac{c_{\mathrm{HW}}}{h_{\mathrm{HW}}} \approx \frac{c_{\mathrm{LW}}}{h_{\mathrm{LW}}} \approx \frac{c}{\bar{h}} \tag{33}$$

$$c_{\mathrm{HW}} + c_{\mathrm{LW}} \approx 2c \tag{34}$$

$$c_{\mathrm{HW}} \approx c\sqrt{1+\zeta} \tag{35}$$

Eq. (35) is Airy's equation (Savenije 2005) provided $c \gg \upsilon\sin(\epsilon)$, which is always the case in alluvial estuaries.

Combining Eqs. (24), (27), and (31) yields the following expression for HW:

$$\frac{r_s c_{\mathrm{HW}}\left[\upsilon\sin(\epsilon) - \frac{Q_f}{A}\right]}{g(\bar{h}+\eta)}\frac{dh_{\mathrm{HW}}}{dx} - \frac{c_{\mathrm{HW}}\left[\upsilon\sin(\epsilon) - \frac{Q_f}{A}\right]}{g}\left(\frac{1}{a} - \frac{1}{\eta}\frac{d\eta}{dx}\right) + \frac{dh_{\mathrm{HW}}}{dx} \pm n^2\frac{\left[\upsilon\sin(\epsilon) - \frac{Q_f}{A}\right]^2}{(\bar{h}+\eta)^{4/3}} = -I_b \tag{36}$$

The last term is the friction term, which has a positive value if $\upsilon\sin(\epsilon) \geq Q_f/A$ and a negative value if $\upsilon\sin(\epsilon) < Q_f/A$.

Similarly, for LW, combination of Eqs. (24), (27), and (32) reads

$$-\frac{r_s c_{\mathrm{LW}}\left[\upsilon\sin(\epsilon) + \frac{Q_f}{A}\right]}{g(\bar{h}-\eta)}\frac{dh_{\mathrm{LW}}}{dx} + \frac{c_{\mathrm{LW}}\left[\upsilon\sin(\epsilon) + \frac{Q_f}{A}\right]}{g}\left(\frac{1}{a} - \frac{1}{\eta}\frac{d\eta}{dx}\right) + \frac{dh_{\mathrm{LW}}}{dx} - n^2\frac{\left[\upsilon\sin(\epsilon) + \frac{Q_f}{A}\right]^2}{(\bar{h}-\eta)^{4/3}} = -I_b \tag{37}$$

Next we introduce the dimensionless tidal amplitude ζ and the dimensionless river discharge term φ:

$$\zeta = \frac{\eta}{\bar{h}} \tag{38}$$

$$\varphi = \frac{Q_f}{A\upsilon\sin(\epsilon)} \tag{39}$$

Subtracting Eqs. (37) and (38), using a Taylor series expansion of $h^{4/3}$, and taking into account the assumption that the wave celerity is symmetrical [Eqs. (33) and (34)] yields the following expressions.

In the downstream tide-dominated zone, where $\varphi \leq 1$,

$$\frac{r_s}{\bar{h}}\left(I - \varphi\frac{d\eta}{dx}\right) - \left(\frac{1}{a} - \frac{1}{\eta}\frac{d\eta}{dx}\right)\theta + \frac{g}{c\upsilon\sin(\epsilon)}\frac{d\eta}{dx} + f\frac{\upsilon\sin(\epsilon)}{c\bar{h}}\left(1 + \varphi^2 + \frac{8}{3}\varphi\zeta\right) = 0 \tag{40}$$

In the upstream river discharge-dominated zone, where $\varphi > 1$,

$$\frac{r_s}{\bar{h}}\left(I - \varphi\frac{d\eta}{dx}\right) - \left(\frac{1}{a} - \frac{1}{\eta}\frac{d\eta}{dx}\right)\theta + \frac{g}{c\upsilon\sin(\epsilon)}\frac{d\eta}{dx} + f\frac{\upsilon\sin(\epsilon)}{c\bar{h}}\left(\frac{4}{3}\zeta + \frac{4}{3}\varphi^2\zeta + 2\varphi\right) = 0 \tag{41}$$

J. Hydraul. Eng. 2012.138:885-896.

with

$$f = \frac{gn^2}{\bar{h}^{1/3}}\left(1 - \left(\frac{4}{3}\zeta\right)^2\right)^{-1} \tag{42}$$

which is the dimensionless friction factor that compensates for the depth not being equal at HW and LW, and

$$\theta = 1 - \frac{c_{HW} - c}{c}\varphi \approx 1 - \left(\sqrt{1+\zeta} - 1\right)\varphi \tag{43}$$

which is the dimensionless term that takes into account the fact that the wave celerity is not equal at HW and LW. Making use of Airy's Eq. (35), this can be made a function of ζ.

Making use of these dimensionless parameters, Eqs. (40) and (41) reduce to the following set of equations

$$\delta = \frac{1}{\eta}\frac{d\eta}{dx}\frac{c_0}{\omega} = \frac{\mu^2}{\mu^2(\theta - r_s\varphi\zeta) + 1}\left[\gamma\theta - \chi\mu^2\lambda^2\left(1 + \varphi^2 + \frac{8}{3}\varphi\zeta\right)\right], \quad \varphi \le 1 \tag{44}$$

$$\delta = \frac{1}{\eta}\frac{d\eta}{dx}\frac{c_0}{\omega} = \frac{\mu^2}{\mu^2(\theta - r_s\varphi\zeta) + 1}\left[\gamma\theta - \chi\mu^2\lambda^2\left(\frac{4}{3}\zeta + \frac{4}{3}\varphi^2\zeta + 2\varphi\right)\right], \quad \varphi > 1 \tag{45}$$

Acknowledgments

The authors would like to thank the three anonymous referees for their valuable comments and suggestions, which have greatly improved this paper.

Notation

The following symbols are used in this paper:

$\bar{A}$ = cross-sectional area of flow;
$\bar{A}_0$ = cross-sectional area at estuary mouth;
a = convergence length of cross-sectional area;
$\bar{B}$ = cross-sectional mean stream width;
$\bar{B}_0$ = width at estuary mouth;
b = convergence length of width;
c = wave celerity;
c_{HW} = wave celerity at HW;
c_{LW} = wave celerity at LW;
c_0 = classical wave celerity;
f = friction factor accounting for difference in friction at HW and LW;
g = acceleration due to gravity;
h = cross-sectional average depth of flow;
h_{HW} = depth at HW;
h_{LW} = depth at LW;
$\bar{h}$ = tidal average depth of flow;
$\bar{h}_0$ = depth at estuary mouth;
I = tidal average water level slope;
I_b = bottom slope;
n = Manning's coefficient;
Q = tidal discharge;
Q_f = river discharge;
r_s = storage width ratio;
T = tidal period;
t = time;
U = cross-sectional average flow velocity;
U_{HW} = tidal velocity at HW;
U_{LW} = tidal velocity at LW;
x = distance;
γ = estuary shape number;
δ = damping number;
ϵ = phase lag;
ζ = tidal amplitude to depth ratio;
η = tidal amplitude;
θ = dimensionless term accounting for wave celerity's not being equal at HW and LW;
λ = celerity number;
μ = velocity number;
υ = tidal velocity amplitude;
φ = dimensionless river discharge term accounting for river discharge;
χ = friction number; and
ω = tidal frequency.

References

Bai, Y. C., Wang, Z. Y., and Shen, H. T. (2003). "Three-dimensional modelling of sediment transport and the effects of dredging in the Haihe Estuary." *Estuar. Coast. Shelf Sci.*, 56(1), 175–186.

Barusseau, J. P. (1998). "Morphological and sedimentological changes in the Senegal River estuary after the constuction of the Diama dam." *J. Afr. Earth Sci.*, 26(2), 317–326.

Blott, S. J., Pye, K., van der Wal, D., and Neal, A. (2006). "Long-term morphological change and its causes in the Mersey Estuary, NW England." *Geomorphology*, 81(1–2), 185–206.

Byun, D. S., Wang, X. H., Hart, D. E., and Cho, Y. K. (2005). "Modeling the effect of freshwater inflows on the development of spring blooms in an estuarine embayment." *Estuar. Coast. Shelf Sci.*, 65(1–2), 351–360.

Edgar, G. J., and Barrett, N. S. (2000). "Effects of catchment activities on macrofaunal assemblages in Tasmanian estuaries." *Estuar. Coast. Shelf Sci.*, 50(5), 639–654.

Friedrichs, C. T., and Aubrey, D. G. (1994). "Tidal propagation in strongly convergent channels." *J. Geophys. Res. Oceans*, 99(C2), 3321–3336.

Godin, G. (1999). "The propagation of tides up rivers with special considerations on the Upper Saint Lawrence River." *Estuar. Coast. Shelf Sci.*, 48(3), 307–324.

Gong, W., and Shen, J. (2011). "The response of salt intrusion to changes in river discharge and tidal mixing during the dry season in the Modaomen Estuary, China." *Cont. Shelf Res.*, 31, 769–788.

Hoa, L. T. V., Nhan, N. H., Wolanski, E., Cong, T. T., and Shigeko, H. (2007). "The combined impact on the flooding in Vietnam's Mekong River delta of local man-made structures, sea level rise, and dams upstream in the river catchment." *Estuar. Coast. Shelf Sci.*, 71(1–2), 110–116.

Horrevoets, A. C., Savenije, H. H. G., Schuurman, J. N., and Graas, S. (2004). "The influence of river discharge on tidal damping in alluvial estuaries." *J. Hydrol.*, 294(4), 213–228.

Hossain, S., Eyre, B. D., and McKee, L. J. (2004). "Impacts of dredging on dry season suspended sediment concentration in the Brisbane River estuary, Queensland, Australia." *Estuar. Coast. Shelf Sci.*, 61(3), 539–545.

Jay, D. A. (1991). "Green's law revisited: Tidal long-wave propagation in channels with strong topography." *J. Geophys. Res. Oceans*, 96(C11), 20585–20598.

Jeuken, M. C. J. L., and Wang, Z. B. (2010). "Impact of dredging and dumping on the stability of ebb-flood channel systems." *Coast. Eng.*, 57(6), 553–566.

Kim, T. I., Choi, B. H., and Lee, S. W. (2006). "Hydrodynamics and sedimentation induced by large-scale coastal developments in the Keum River Estuary, Korea." *Estuar. Coast. Shelf Sci.*, 68(3–4), 515–528.

Lanzoni, S., and Seminara, G. (1998). "On tide propagation in convergent estuaries." *J. Geophys. Res. Oceans*, 103(C13), 30793–30812.

J. Hydraul. Eng. 2012.138:885-896.

Li, M. G. (2010). "The effect of reclamation in areas between islands in a complex tidal estuary on the hydrodynamic sediment environment." *J. Hydrodyn.*, 22(3), 338–350.
Liria, P., Garel, E., and Uriarte, A. (2009). "The effects of dredging operations on the hydrodynamics of an ebb tidal delta: Oka Estuary, northern Spain." *Cont. Shelf Res.*, 29(16), 1983–1994.
Luo, X. L., Zeng, E. Y., Ji, R. Y., and Wang, C. P. (2007). "Effects of in-channel sand excavation on the hydrology of the Pearl River Delta, China." *J. Hydrol.*, 343(3–4), 230–239.
Nguyen, A. D., and Savenije, H. H. G. (2006). "Salt intrusion in multi-channel estuaries: A case study in the mekong delta, vietnam." *Hydrol. Earth Syst. Sci.*, 10(5), 743–754.
Punt, A. G., Millward, G. E., and Harris, J. R. W. (2003). "Modelling solute transport in the Tweed Estuary, UK using ECoS." *Sci. Total Environ.*, 314–316(0), 715–725.
Savenije, H. H. G. (1992). "Lagrangian solution of St. Venant's equations for alluvial estuary." *J. Hydraul. Eng.*, 118(8), 1153–1163.
Savenije, H. H. G. (1993). "Determination of estuary parameters on basis of Lagrangian analysis." *J. Hydraul. Eng.*, 119(5), 628–642.
Savenije, H. H. G. (1998). "Analytical expression for tidal damping in alluvial estuaries." *J. Hydraul. Eng.*, 124(6), 615–618.
Savenije, H. H. G. (2001). "A simple analytical expression to describe tidal damping or amplification." *J. Hydrol.*, 243(3–4), 205–215.
Savenije, H. H. G. (2005). *Salinity and tides in alluvial estuaries*, Elsevier, New York, 23–107.
Savenije, H. H. G., Toffolon, M., Haas, J., and Veling, E. J. M. (2008). "Analytical description of tidal dynamics in convergent estuaries." *J. Geophys. Res. Oceans*, 113(C10), 18.
Savenije, H. H. G., and Veling, E. J. M. (2005). "Relation between tidal damping and wave celerity in estuaries." *J. Geophys. Res. Oceans*, 110(C4), 10.
Smith, A. M., Wood, A. C. L., Liddy, M. F. A., Shears, A. E., and Fraser, C. I. (2010). "Human impacts in an urban port: The carbonate budget, Otago Harbour, New Zealand." *Estuar. Coast. Shelf Sci.*, 90(2), 73–79.
Smith, R., Boyd, S. E., Rees, H. L., Dearnaley, M. P., and Stevenson, J. R. (2006). "Effects of dredging activity on epifaunal communities-surveys following cessation of dredging." *Estuar. Coast. Shelf Sci.*, 70(1–2), 207–223.
Toffolon, M., and Savenije, H. H. G. (2011). "Revisiting linearized one-dimensional tidal propagation." *J. Geophys. Res. Oceans*, 116(C07007), 13.
Van Rijn, L. (2011). "Analytical and numerical analysis of tides and salinities in estuaries. I: Tidal wave propagation in convergent estuaries." *Ocean Dyn.*, 61(11), 1719–1741.
Xie, D. F., Wang, Z. B., Gao, S., and De Vriend, H. J. (2009). "Modeling the tidal channel morphodynamics in a macro-tidal embayment, Hangzhou Bay, China." *Cont. Shelf Res.*, 29(15), 1757–1767.
Zhang, W., Ruan, X. H., Zheng, J. H., Zhu, Y. L., and Wu, H. X. (2010). "Long-term change in tidal dynamics and its cause in the Pearl River Delta, China." *Geomorphology*, 120(3–4), 209–223.
Zhang, W., Yan, Y. X., Zheng, J. H., Li, L., Dong, X., and Cai, H. J. (2009). "Temporal and spatial variability of annual extreme water level in the Pearl River Delta region, China." *Global Planet. Change*, 69(1–2), 35–47.

J. Hydraul. Eng. 2012.138:885-896.